Aqueous Chemistry of High-Valent Manganese. Structure, Magnetic, and Redox Properties of a New Type of Mn-Oxo Cluster, $[Mn^{IV}_4O_6(bpy)_6]^{4+}$: Relevance to the Oxygen Evolving Center in Plants

Christian Philouze,[1a] Geneviève Blondin,[1a] Jean-Jacques Girerd,*[,1a] Jean Guilhem,[1b] Claudine Pascard,[1b] and Doris Lexa[1c]

Contribution from the Laboratoire de Chimie Inorganique, URA CNRS 420, Institut de Chimie Moléculaire d'Orsay, Université Paris-Sud, 91405 Orsay, France, Institut de Chimie des Substances Naturelles, UPR CNRS 2301, 91198 Gif-sur-Yvette, France, and Laboratoire d'Electrochimie Moléculaire, URA CNRS 438, Université Paris VII, 75251 Paris, France

Received February 14, 1994®

Abstract: The tetranuclear species $[Mn^{IV}_4O_6(bpy)_6](ClO_4)_4\cdot H_2O$ was isolated from an aqueous nitric acid solution (pH = 2) of $Mn^{III}(bpy)Cl_3(H_2O)$ upon addition of $NaClO_4$. It crystallizes in the triclinic space group $P\bar{1}$ with a = 20.213(7) Å, b = 13.533(7) Å, c = 13.411(8) Å, α = 112.01(8)°, β = 96.72(11)°, γ = 100.34(12)°, V = 3276.9 Å^3, and Z = 2. The cation has a nonrectilinear chain structure $[(bpy)_2Mn^{IV}_aO_2Mn^{IV}_b(bpy)O_2Mn^{IV}_c(bpy)O_2Mn^{IV}_d(bpy)_2]^{4+}$. The metal–metal distances are Mn_a–Mn_b = 2.746(5) Å, Mn_b–Mn_c = 2.760(5) Å, Mn_c–Mn_d = 2.735(4) Å, Mn_a–Mn_c = 4.899(10) Å, Mn_b–Mn_d = 4.897(6) Å, and Mn_a–Mn_d = 6.419(11) Å. The variable temperature magnetic susceptibility data for $[Mn^{IV}_4O_6(bpy)_6](ClO_4)_4\cdot H_2O$ in the range 12–294 K were fit using the spin Hamiltonian $H_S = -J_{ab}S_aS_b - J_{bc}S_bS_c - J_{cd}S_cS_d$, with $J_{ab} = J_{cd} = -176$ cm^{-1} and $J_{bc} = -268$ cm^{-1}. The lowest spin states are organized similarly to those for a dinuclear Mn^{IV}–Mn^{IV} unit. This is due to the stronger antiferromagnetic coupling between the two central Mn^{IV} ions relative to the coupling between a and b on one hand and c anc d on the other hand. This compound is EPR inactive at 4 K but shows a spectrum around 100 K which was attributed to the triplet and quintet excited states. Electrochemically, the cation $[Mn^{IV}_4O_6(bpy)_6]^{4+}$ is irreversibly reduced to Mn^{II} at +0.5 V/SCE. Its lower oxidizing power than those of $[Mn^{IV}_2O_2L_4]^{4+}$ (L = bpy or phen) was attributed to the dispersion of the positive charge and the surrounding of Mn^{IV} central ions by oxo groups. The $[Mn^{IV}_4O_6(bpy)_6]^{4+}$ differs by the nature of the central bridge from the proposal by Klein et al. (*Science* **1993**, *260*, 675–679) for the structure of the oxygen evolving center (OEC) in plants. In the hypothesis that in the S_2 state, the oxidation state of the OEC is $Mn^{IV}_3Mn^{III}$, the cation $[Mn^{IV}_4O_6(bpy)_6]^{4+}$ would correspond at least formally to the S_3 state. Both $[Mn^{IV}_4O_6(bpy)_6]^{4+}$ and Klein's model have the same spin coupling chain topology. We thus applied our results on spin coupling in $[Mn^{IV}_4O_6(bpy)_6]^{4+}$ to the spin coupling properties of the S_2 state of the OEC. We showed that in order to interpret the ground state observed for the pre-S_2 and S_2 states, Klein's model has to be adapted in either of the two following possibilities. (i) The "short–short–long" model, which has the metal–metal bond distances reordered as Mn_a–Mn_b = 2.7 Å, Mn_b–Mn_c = 2.7 Å, Mn_c–Mn_d = 3.3 Å. The distribution of oxidation states along abcd is then (IV,III,IV,IV). Depending on the sign of J_{cd}, this model has a $S = {}^1/_2$ (J_{cd} antiferro) or a $S = {}^5/_2$ ground state (J_{cd} ferro). This model could be dismissed if it would be proven that the g = 4.1 signal originates from a $S = {}^3/_2$ ground state. (ii) The "ring" model. By analyzing the exact solutions of the ring spin coupling problem $H_S = -J_{ab}S_aS_b - J_{bc}S_bS_c - J_{cd}S_cS_d - J_{da}S_dS_a$, we showed that such a ring model with $J_{ab} = J_{cd} < 0$, $J_{bc} < 0$, and $J_{da} > 0$ can have a ground state with $S = {}^1/_2$, ${}^3/_2$, or ${}^5/_2$, depending on J_{da}/J_{ab} and J_{bc}/J_{ab}. For instance, with $S_a = 2$, $S_b = S_c = S_d = {}^3/_2$, and $J_{bc}/J_{ab} = 1$, a ratio $J_{da}/J_{ab} = -0.35$ is necessary to get $S = {}^3/_2$, which implies the existence of an efficient coupling group between the two terminal manganese atoms.

Introduction

Research on the catalytic role of manganese in water oxidation by the oxygen evolving center (OEC) of Photosystem II (PS II) of plants is particularly active and mobilizes several techniques.[2] The OEC contains four Mn atoms.[2] Its function is to oxidize two water molecules into O_2, following the equation

$$2H_2O \rightarrow O_2 + 4H^+ + 4e^-$$

The oxidizing equivalents are generated one by one by the photosynthetic reaction center. During this process, the cluster goes through five oxidation states S_{0-4}, the index of which refers to the number of oxidizing equivalents stored.

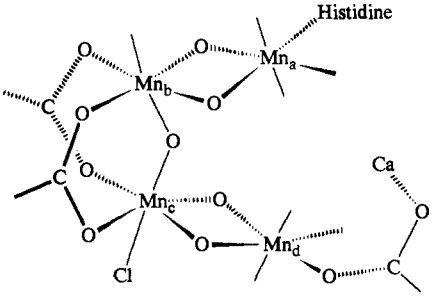

Figure 1. Klein's model for the OEC (adapted from ref 3).

Recently, Klein et al.[3] have from their EXAFS experiments proposed a structural model which is summarized in Figure 1. The site would contain two di-μ-oxo units linked by a μ-oxo-

* Abstract published in *Advance ACS Abstracts,* August 15, 1994.

(1) (a) Université Paris-Sud. (b) Institut de Chimie des Substances Naturelles. (c) Université Paris VII.

(2) For reviews, see: Debus, R. J. *Biochim. Biophys. Acta* **1992**, *1102*, 269–352. Rutherford, A. W.; Zimmerman, J.-L.; Boussac, A. In *The Photosystems: Structure, Function and Molecular Biology*; Barber, J., Ed.; Elsevier Science Publishers: New York, 1992; Chapter 5, pp 179–229.

(3) Yachandra, V. K.; DeRose, V. J.; Latimer, M. J.; Mukerji, I.; Sauer, K.; Klein, M. P. *Science* **1993**, *260*, 675–679.

0002-7863/94/1516-8557$04.50/0

bis-μ-carboxylate bridge. The Mn–Mn distances would be Mn_a–Mn_b = Mn_c–Mn_d = 2.7 Å and Mn_b–Mn_c = 3.3 Å.

EPR experiments have also been a major source of information on the OEC since the discovery by Dismukes and Siderer in 1981 of a multiline signal centered close to $g = 2$ for the S_2 state.[4] This signal was observed below 35 K on PS II particles after continuous illumination at intermediate temperatures (between 160 and 200 K).[5] The multiline aspect is due to hyperfine coupling and undoubtedly shows that the signal comes from a manganese cluster ($I_{55_{Mn}} = {}^5/_2$). Recently it has been shown that this multiline signal arises from a $S = {}^1/_2$ ground state.[6] Interpretation of the hyperfine couplings observed strongly suggests that this $S = {}^1/_2$ state is issued from a cluster made of the four manganese atoms.[7,8] This imposes that the cluster contains an odd number of unpaired electrons, so that the oxidation states must be $Mn^{IV}_3Mn^{III}$ or $Mn^{IV}Mn^{III}_3$. From XANES measurements, the former is favored.[3] When the PS II particles are illuminated at 140 K, the signal observed is centered close to $g = 4.1$.[9,10] This signal is considered to originate from a $S = {}^3/_2$[11,12,13] or a $S = {}^5/_2$ ground state.[14] The observation of a multiline structure on this $g = 4.1$ signal proves that it arises from a manganese cluster.[15] The $g = 2$ and $g = 4.1$ signals would come from two different conformations of the Mn_4 cluster in the same oxidation state.[16,17] A signal has been observed in the S_3 state of Ca-depleted PS II particles.[18] It has been interpreted as issued from the coupling between a histidine cation radical and the Mn_4 cluster in its $S = {}^1/_2$ ground state.[19] The implication of oxidation of an amino acid would lead to the idea that the oxidizing equivalents are not all stored on manganese atoms.[20] As outlined above, this system is very sophisticated, and some time will be necessary before a complete understanding is attained.

Bioinorganic chemists can contribute to the solution of this problem by synthesizing Mn clusters and comparing the electronic properties of these models to the OEC (see refs 21 and 22 for reviews). Recently an interesting proposal by Pecoraro for the mechanism of water oxidation has been published.[22]

Since the beginning of the study of the OEC, one key model compound has been the dinuclear unit $[(bpy)_2Mn^{III}O_2Mn^{IV}(bpy)_2]^{3+}$ obtained in 1960 by Nyholm and Turco[23] and structurally characterized in 1972 by Plaskin et al.[24] This system has been studied in detail by Calvin et al.[25,26] It has a $S = {}^1/_2$ ground state arising from the antiferromagnetic coupling between the spins of the Mn^{III} (high spin, $S_a = 2$) and the Mn^{IV} ($S_b = {}^3/_2$) ions. The electronic wave function of this ground state is noted $|S_a = 2, S_b = {}^3/_2, S = {}^1/_2\rangle$. This state gives an EPR spectrum composed of 16 lines centered on $g = 2$; these lines originate from the hyperfine coupling between the electronic spin and the nuclear spins of the two Mn nuclei. This is the simplest polynuclear Mn compound having a $S = {}^1/_2$ ground state, and, as such, it has been intensively studied as a model for the multiline $g = 2$ OEC EPR signal. The Mn–Mn distance in this compound is 2.716 Å,[24] and this compound has also been a structural model for EXAFS studies. Both X-ray diffraction[24] and EPR[26] demonstrate that the valences are localized. This localization is due to the Jahn–Teller effect around the Mn^{III}, which manifests itself by a strong distorsion with the axial distances elongated. The Mn^{III} ion is in a $d_{\pi}{}^3d_{z^2}{}^1$ ground state with the z axis perpendicular to the Mn_2O_2 plane. This is quite general for $[Mn^{III}O_2Mn^{IV}]^{3+}$ systems.[27] This orientation of the orbital holding the extra electron on Mn^{III} certainly does not favor its delocalization on the neighboring site.

Curiously, it was only in 1990 that another cluster was isolated in the $Mn^{III,IV}$-bpy system. We isolated the triangular $[Mn^{IV}_3O_4(bpy)_4Cl_2]^{2+}$ cation[28] and Brudvig the triangular $[Mn^{IV}_3O_4(bpy)_4(H_2O)_2]^{4+}$ unit.[29] These species have an EPR spectrum[28,29] containing 35 lines coming from hyperfine coupling. It demonstrates that the ground state is the $|(S_a = {}^3/_2, S_b = {}^3/_2)\ S_{ab} = 1, S_c = {}^3/_2, S = {}^1/_2\rangle$ state arising from the antiferromagnetic coupling of the spins of the three Mn^{IV} (S_i notes the spin of the i^{th} Mn^{IV} ion, $S_i = {}^3/_2$, and S is the total spin). This spectrum is not encountered in the OEC.[2] One interesting feature of the structure of these species is that they show distances Mn–Mn = 2.7 and 3.3 Å comparable to those found in OEC, but the EXAFS spectrum is quite different from the OEC one as far as the intensities of the corresponding peaks are concerned: for the OEC, the ratio of the intensities of the 2.7 and the 3.3 Å peaks is much larger than in these models.[30]

The $[Mn^{IV}_3O_4(bpy)_4(H_2O)_2]^{4+}$ cation was isolated in aqueous solution of $[(bpy)_2Mn^{III}O_2Mn^{IV}(bpy)_2]^{3+}$ at low pH (<1.5). We were able to get $[Mn^{IV}_3O_4(bpy)_4(H_2O)_2]^{4+}$ starting from the mononuclear $Mn^{III}(bpy)Cl_3(H_2O)$[41] species.[31] We systematically explored the influence of pH on these reactions of disproportionation and condensation in water, and we isolated the new species $[Mn^{IV}_4O_6(bpy)_6]^{4+}$.[32]

The chemistry of $Mn^{III,IV}$-byp-AcO[33,34,35,36] or $Mn^{III,IV}$-bpy-phosphato[37,38] systems is equally rich.

The $Mn^{III,IV}$-phen system was also explored. The $[(phen)_2Mn^{III}O_2Mn^{IV}(phen)_2]^{3+}$ and $[(phen)_2Mn^{IV}O_2Mn^{IV}(phen)_2]^{4+}$ systems have been prepared[25,38] and studied in great detail by

(4) Dismukes, G. C.; Siderer, Y. *Proc. Natl. Acad. Sci. U.S.A.* **1981**, *78*, 274–278.
(5) Brudvig, G. W.; Casey, J. L.; Sauer, K. *Biochim. Biophys. Acta* **1983**, *723*, 366–371.
(6) Britt, R. D.; Lorigan, G. A.; Sauer, K.; Klein, M. P.; Zimmermann, J.-L. *Biochim. Biophys. Acta* **1992**, *1040*, 95–101.
(7) Kusunoki, M. *Chem. Phys. Lett.* **1992**, *197*, 108.
(8) Bonvoisin, J.; Blondin, G.; Girerd, J.-J.; Zimmermann, J.-L. *Biophys. J.* **1992**, *61*, 1076–1086.
(9) Casey, J. L.; Sauer, K. *Biochim. Biophys. Acta* **1984**, *767*, 21–28.
(10) Zimmermann, J.-L.; Rutherford, A. W. *Biochim. Biophys. Acta* **1984**, *767*, 160–167.
(11) Hansson, Ö.; Aasa, R.; Vänngard, T. *Biophys. J.* **1987**, *51*, 825.
(12) Smith, P. J.; Ahrling, K. A.; Pace, R. J. *J. Chem. Soc., Faraday Trans. 1* **1993**, *89*, 2863–2868.
(13) de Paula, J. C.; Beck, W. F.; Miller, A. F.; Wilson, R. B.; Brudvig, G. W. *J. Chem. Soc., Faraday Trans. 1* **1987**, *83*, 3635.
(14) Haddy, A.; Dunham, W. R.; Sands, R. H.; Aasa, R. *Biochim. Biophys. Acta* **1992**, *1099*, 25–34.
(15) Kim, D. H.; Britt, R. D.; Klein, M. P.; Sauer, K. *J. Am. Chem. Soc.* **1990**, *112*, 9389.
(16) de Paula, J. C.; Beck, W. F.; Brudvig, G. W. *J. Am. Chem. Soc.* **1986**, *108*, 4002–4009.
(17) Zimmermann, J.-L.; Rutherford, A. W. *Biochemistry* **1986**, *25*, 4609–4615.
(18) Boussac, A.; Zimmermann, J.-L.; Rutherford, A. W. *Biochemistry* **1989**, *28*, 8984–8989.
(19) Boussac, A.; Zimmermann, J.-L.; Rutherford, A. W. *Nature* **1990**, *347*, 303–306.
(20) This proposal has been made by several authors. See ref 2.
(21) Wieghardt, K. *Angew. Chem., Int. Ed. Engl.* **1989**, *28*, 1153–1172. Vincent, J. B.; Christou, G. *Adv. Inorg. Chem.* **1989**, *33*, 197–257.
(22) *Manganese Red-Ox Enzymes*; Pecoraro, V. L., Ed.; VCH: New York, 1992.
(23) Nyholm, R. S.; Turco, A. *Chem. Ind. (London)* **1960**, 74.
(24) Plaskin, P. M.; Stoufer, R. C.; Mathew, M.; Palenik, G. J. *J. Am. Chem. Soc.* **1972**, *94*, 2121–2122.
(25) Cooper, S. R.; Calvin, M. *J. Am. Chem. Soc.* **1977**, *99*, 6623–6630.
(26) Cooper, S. R.; Dismukes, G. C.; Klein, M. P.; Calvin, M. *J. Am. Chem. Soc.* **1978**, *100*, 7248–7252.
(27) Tan, X.; Gultneh, Y.; Sarneski, J. E.; Scholes, C. P. *J. Am. Chem. Soc.* **1991**, *113*, 7853–7858. Tang, X. S.; Sivaraja, M.; Dismukes, C. *J. Am. Chem. Soc.* **1993**, *115*, 2382–2389.
(28) Auger, N.; Girerd, J.-J.; Corbella, M.; Gleizes, A.; Zimmermann, J.-L. *J. Am. Chem. Soc.* **1990**, *112*, 448–450.
(29) Sarneski, J. E.; Thorp, H. H.; Brudvig, G. W.; Crabtree, R. H.; Schulte, G. K. *J. Am. Chem. Soc.* **1990**, *112*, 7255–7260.
(30) Auger, N.; Girerd, J.-J.; Klein, M. P., unpublished results.
(31) Auger, N.; Girerd, J.-J., unpublished results.
(32) Philouze, C.; Blondin, G.; Ménage, S.; Auger, N.; Girerd, J.-J.; Vigner, D.; Lance, M.; Nierlich, M. *Angew. Chem., Int. Ed. Engl.* **1992**, *31*, 1629–1631.
(33) Machandra, R.; Brudvig, G. W.; Crabtree, R. H.; Sarneski, J. E.; Didiuk, M. *Inorg. Chim. Acta* **1993**, *212*, 135–137.
(34) Dave, B. C.; Czenuszewicz, R. S.; Bond, M. R.; Carrano, C. J. *Inorg. Chem.* **1993**, *32*, 3593–3594.
(35) Ménage, S.; Girerd, J.-J.; Gleizes, A. *J. Chem. Soc., Chem. Commun.* **1988**, 431.
(36) Christou, G. *Acc. Chem. Res.* **1989**, *22*, 328.
(37) Sarneski, J. E.; Didiuk, M.; Thorp, H. H.; Crabtree, R. H.; Brudvig, G. W.; Faller, Schulte, G. K. *Inorg. Chem.* **1991**, *30*, 2835–2836.
(38) Goodwin, H. A.; Sylva, R. N. *Aust. J. Chem.* **1967**, *20*, 629–637.

radiocrystallography.[39] We prepared $[Mn^{IV}_3O_4(phen)_4(H_2O)_2]^{4+}$ by hydrolysis[40] of $Mn^{III}(phen)Cl_3(H_2O)$.[41] We could get the tetranuclear species.

The electrochemistry of the dinuclear phen and bpy systems in acetonitrile has allowed the identification of the couples E^0-[IV,IV]/[III,IV] = 1.2 V/SCE and E^0[III,IV]/[III,III] = 0.3 V/SCE.[25] The electrochemistry in aqueous solution of the same systems has been thoroughly studied by Thorp et al.[42] who characterized at pH > 2 the couples $E^0[Mn^{III}O_2Mn^{IV}]/[Mn^{III}O(OH)Mn^{III}]$ = 0.85 – 0.06 (pH – 2) V for bpy and $E^0[Mn^{III}O_2Mn^{IV}]/[Mn^{III}O(OH)Mn^{III}]$ = 0.9 – 0.06 (pH – 2) V and $E^0[Mn^{III}O(OH)Mn^{III}]/[Mn^{III}(OH)_2Mn^{II}]$ = 0.25 – 0.06 (pH – 2) V for phen. All potentials are given versus SCE. Protonation of one of the oxo groups of the [III,III] species significantly increases the potential of the [III,IV] species.

We report here the detailed study of $[Mn^{IV}_4O_6(bpy)_6]^{4+}$. A preliminary report appeared in ref 32.

Experimental Section

$Mn(bpy)Cl_3(H_2O)$ was synthesized as in ref 41.

Synthesis. $Mn(bpy)Cl_3(H_2O)$ (0.2 g, 0.59 mmol) was dissolved in small portions and under stirring in 15 mL of a pH = 2.0 nitric acid solution. The pH was controlled with a pH meter during the addition and maintained at 2.0 by addition of a few drops of a sodium hydroxide solution (5 M). When the addition was complete, the mixture was centrifuged and filtered to eliminate the manganese hydroxide which had precipitated. Sodium perchlorate (0.146 g, 1.19 mmol) was added with stirring to the filtrate. The solution was set to crystallize, and within a few days, dark-brown crystals of $[Mn^{IV}_4O_6(bpy)_6][ClO_4)_4\cdot H_2O$ appeared (yield, 30% based on Mn). Freshly prepared crystals contain $2H_2O$ per tetranuclear unit. One water molecule is easily lost. Calcd for $C_{60}H_{52}Cl_4Mn_4N_{12}O_{24}$: C, 42.73; H, 3.08; N, 9.97; Cl, 8.41; Mn, 13.03. Found: C, 42.23; H, 3.06; N, 9.88; Cl, 8.72; Mn, 12.94.

Electrochemistry. (a) Cyclic Voltammetry. Cyclic voltammetry was measured using an home-made potentiostat and a current measurer equipped with a positive feedback ohmic drop compensation, a Parr (175) function generator, and a X–Y chart recorder (IFELEC 2502). As working electrode, glassy carbon (Tokai, Japan; Φ = 3 mm) provided the best results. It was carefully polished with diamond pastes and ultrasonically rinsed in ethanol before each potential run. An Au wire as auxiliary electrode and a saturated calomel electrode separated by a fritted disk from the main solution as reference were used. The experiments were carried out in a double-wall Pyrex cell (thermostated with 2-propanol) on carefully degassed solutions by argon flushing.

(b) Preparative Scale Electrolysis. This was carried out on a large glassy carbon electrode with the same reference electrode and a larger auxiliary electrode separated from the bulk solution by a large fritted disk. The charges were measured with a Tacussel IGN 5 integrator and the intensity with an amperemeter Peckly Didact A430. The potential was imposed with an home-made potentiostat (50 V, 1 A) and controlled with a millivoltmeter AOIP MNK79.

Magnetic Susceptibility Measurements. Magnetic susceptibility measurements in the 12-300 K temperature range were carried out with a Faraday-type magnetometer equipped with a helium continuous-flow catalyst. Automatic data acquisition equipment was made at the Laboratoire de Chimie Inorganique. $HgCo(NCS)_4$ was used as a susceptibility standard.

Crystallographic Data Collection and Refinement of the Structure. A crystal (0.3 × 0.3 × 0.4 mm^3) was mounted on a Philips PW 1100 diffractometer using graphite monochromated Mo Kα radiation. The main crystallographic data are given in Table 1. The data collection was performed with the following scanning conditions: $\omega/2\theta$ mode, up to six scans, speed 0.1 deg s^{-1}, width 1.2°. The structure was solved with SHELX86 and refined with SHELX76 programs.[43,44] Owing to the small number of data, we tried to limit the number of parameters. The refinement was started using rigid blocks for pyridine and perchlorate groups. The following strategy was adopted: chemically equivalent distances in the organic part of the molecule were tied to only one parameter.[45] Anisotropic temperature coefficients were used only for Mn, O, and Cl atoms; H atom positions were calculated (C–H = 1 Å). Despite the presence of two disordered perchlorate anions on or near to the centers of symmetry, we performed the refinement in the $P\bar{1}$ and not in the $P1$ space group. The weighting scheme is $w = [\sigma^2(F) + 0.008F^2]^{-1}$.

Table 1. Crystallographic Data for $[Mn_4O_6(bpy)_6](ClO_4)_4\cdot H_2O$

formula	$C_{60}H_{50}Cl_4Mn_4N_{12}O_{23}$
FW	1668.68
radiation	Mo Kα
temp, K	294
space group	$P\bar{1}$
a, Å	20.213(7)
b, Å	13.533(7)
c, Å	13.411(8)
α, deg	112.01(8)
β, deg	96.72(11)
γ, deg	100.34(12)
V, Å^3	3276.9
Z	2
μ, mm^{-1}	0.97
N_{meas}	6507
N_{obs} [$2\sigma(I)$]	2214
R	4.8
R_w	5.9

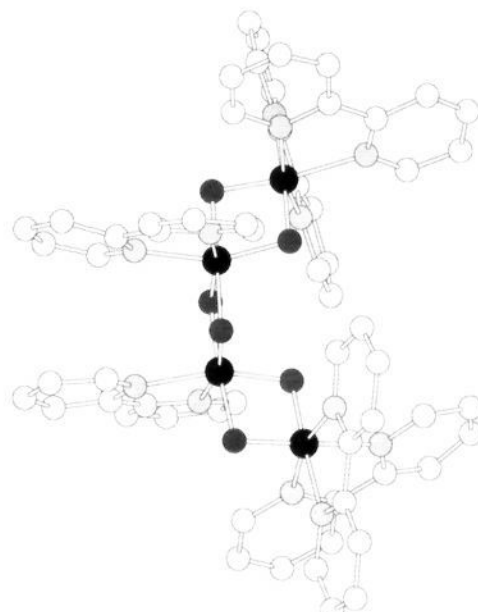

Figure 2. Structure of $[Mn^{IV}_4O_6(bpy)_6]^{4+}$ showing the atom-labeling scheme. Hydrogen atoms are omitted.

EPR Spectra. EPR spectra were recorded on a Bruker ER 200 D spectrometer at X-band fitted with an Oxford continuous-flow liquid helium cryostat, a temperature control system, and a microwave frequency meter HP 5350 B.

Results and Discussion

Structure. The structure of the $[Mn_4O_6(bpy)_6]^{4+}$ cation is represented in Figure 2. It consists of a pair of dimanganese-di-μ-oxo units bridged by two μ-oxo anions. This is the first example of the linear $[Mn_4O_6]^{4+}$ core. The core with the coordinated nitrogen atoms is represented in Figure 3. Selected distances are indicated in Table 2. The Mn^{IV}–Mn^{IV} distances between nearest neighbors are Mn_a–Mn_b = 2.746(5) Å, Mn_b–

(39) Stebler, M.; Ludi, A.; Bürgi, H.-B. *Inorg. Chem.* **1986**, *25*, 4743–4750.
(40) Auger, N.; Philouze, C.; Girerd, J.-J., unpublished results.
(41) Goodwin, H. A.; Sylva, R. N. *Aust. J. Chem.* **1965**, *18*, 1742–1749.
(42) Machandra, R.; Thorp, H. H.; Brudvig, G.; Crabtree, R. H. *Inorg. Chem.* **1992**, *31*, 4040–4041. Thorp, H. H.; Sarneski, J. E.; Brudvig, G. W.; Crabtree, R. H. *J. Am. Chem. Soc.* **1989**, *111*, 9249.
(43) Sheldrick, G. M. *SHELXS86*, Program for Crystal Structure Solution; University of Göttingen: Göttingen, Germany, 1986.
(44) Sheldrick, G. M. *SHELX76*, Program for Crystal Structure Solution; University of Cambridge: Cambridge, England, 1976.
(45) Waser, J. *Acta Crystallogr.* **1963**, *16*, 1091–1094.

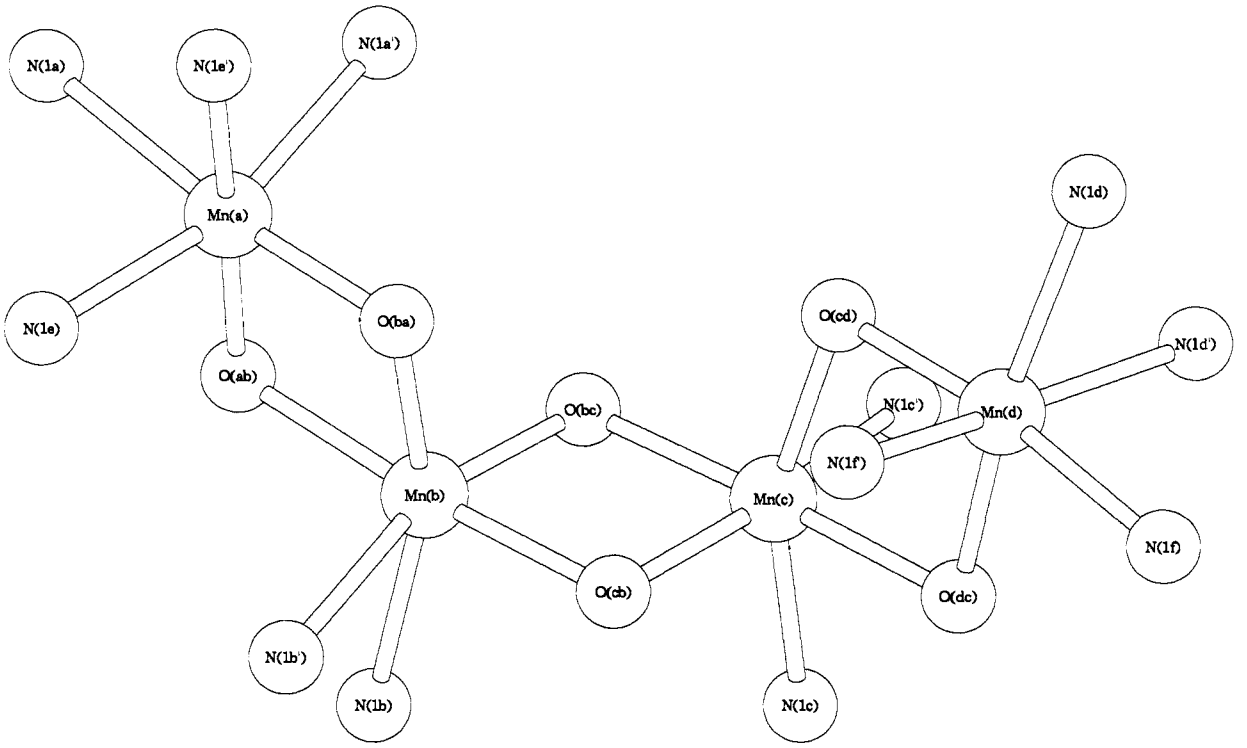

Figure 3. Structure of $[Mn^{IV}_4O_6(bpy)_6]^{4+}$ with only the atoms directly coordinated to Mn atoms shown.

Table 2. Selected Bond Lengths (Å) and Angles (deg) for $[Mn_4O_6(bpy)_6](ClO_4)_4 \cdot H_2O$

	Lengths		
Mn_aO_{ab}	1.753(10)	Mn_bO_{ab}	1.910(10)
Mn_aO_{ba}	1.743(9)	Mn_bO_{ba}	1.823(11)
Mn_aN_{1a}	2.122(12)	Mn_bO_{bc}	1.815(10)
$Mn_aN_{1a'}$	2.034(12)	Mn_bO_{cb}	1.851(9)
Mn_aN_{1e}	2.021(12)	Mn_bN_{1b}	2.096(12)
$Mn_aN_{1e'}$	2.062(13)	$Mn_bN_{1b'}$	2.127(12)
Mn_cO_{cd}	1.847(11)	Mn_dO_{cd}	1.768(11)
Mn_cO_{dc}	1.014(9)	Mn_dO_{dc}	1.791(10)
Mn_cO_{bc}	1.879(10)	Mn_dN_{1d}	2.109(13)
Mn_cO_{cb}	1.792(10)	$Mn_dN_{1d'}$	2.026(12)
Mn_cN_{1c}	2.041(13)	Mn_dN_{1f}	2.092(12)
$Mn_cN_{1c'}$	2.098(12)	Mn_dN_{1f}	2.018(12)
Mn_a–Mn_b	2.746(5)		
Mn_b–Mn_c	2.760(5)		
Mn_c–Mn_d	2.735(4)		
Mn_a–Mn_c	4.899(10)		
Mn_b–Mn_d	4.897(6)		
Mn_a–Mn_d	6.419(11)		
	Angles		
Mn_a–Mn_b–Mn_c	125.66(16)	Mn_b–O_{bc}–Mn_c	96.7(5)
Mn_b–Mn_c–Mn_d	126.07(12)	Mn_b–O_{cb}–Mn_c	98.5(5)
Mn_a–Mn_b–Mn_c–Mn_d	64.0(1)	Mn_c–O_{cd}–Mn_d	98.3(5)
Mn_a–O_{ab}–Mn_b	97.0(5)	Mn_c–O_{dc}–Mn_d	95.1(5)
Mn_a–O_{ba}–Mn_b	100.7(5)		

Mn_c = 2.760(5) Å, and Mn_c–Mn_d = 2.735(4) Å. These are typical. In $[Mn_2O_2(phen)_4]^{4+}$, this distance is 2.748(2) Å.[39] In $[Mn_3O_4]^{4+}$ cores, the dimanganese di-μ-oxo pair shows slightly shorter distances: 2.681(3),[28] or 2.679 Å.[29] This seems to be due to the presence of the $(bpy)_2MnO_2$ extra bridge, which tends to bring closer the two Mn atoms of the di-μ-oxo pair. The same effect is observed in $[Mn_2O_2AcO]^{3+}$, where an acetato group bridges the two Mn^{IV} ions (2.642 Å),[34] and in $[Mn_2O_2HPO_4]^{2+}$ (2.702 Å).[37]

The tetranuclear unit can be built from the $Mn_bO_2Mn_c$ core. One extra Mn^{IV} ion (for example, Mn_a) is linked to one side of this core through two oxo groups in a cis mode. This leads to one short axial bond, Mn_b–O_{ba} = 1.823(11) Å, and a long equatorial one, Mn_b–O_{ab} = 1.910(10) Å. This long distance is due to the trans effect of the O_{cb} group. Reciprocally, the Mn_b–O_{cb} = 1.851(9) Å bond is also elongated. This leads to a deformation of the central $Mn_bO_{bc}O_{cb}Mn_c$ motif: Mn_b–O_{bc} = 1.815(10) Å, Mn_c–O_{cb} = 1.792(10) Å, and Mn_c–O_{bc} = 1.879(10) Å. This deformation indeed does not exist in $[Mn_2O_2(phen)_4]^{4+}$, in which the Mn–O distances are between 1.797(3) and 1.805(3) Å.[39]

The fourth Mn atom (Mn_d) is linked to the core in the same half-space as Mn_a relative to the $Mn_bO_2Mn_c$ basal plane but in such a way that a pseudo-C_2 axis perpendicular to the Mn_bO_2-Mn_c plane is obeyed. The Mn_a–Mn_b–Mn_c–Mn_d arrangement is not rectilinear: the angles are Mn_a–Mn_b–Mn_c = 125.66(16)° and Mn_b–Mn_c–Mn_d = 126.07(12)°, and the torsion angle is Mn_a–Mn_b–Mn_c–Mn_d = 64.0(1)°. The distances between next-nearest neighbors are Mn_a–Mn_c = 4.899(10) Å and Mn_b–Mn_d = 4.897(6) Å. The distance between the terminal atoms is Mn_a–Mn_d = 6.419(11) Å.

The distances between the terminal Mn atoms and the oxo groups are between 1.743(9) and 1.791(10) Å and are comparable to those in $[Mn_2O_2(phen)_4]^{4+}$.[39] The octahedral coordination is completed by nitrogen atoms. Mn–N distances trans to the oxo groups are between 2.041(13) and 2.127(12) Å. The others are shorter (2.018(12)–2.034(12) Å). This was already noted by Stebler et al.[39] in the structure of $[Mn_2O_2(phen)_4]^{4+}$.

Synthesis. The obtention of this tetrameric system in the already rich, high-valent manganese bpy aqueous system was a surprise. From this work and works from other groups, one can tentatively rationalize this chemistry by the following equations. Ligand water molecules have been omitted for clarity.

Hydrolysis of $Mn^{III}(bpy)Cl_3(H_2O)$ at pH = 5 gives $[Mn^{III,IV}_2O_2(bpy)_4]^{3+}$. The first step is a condensation reaction:

$$2Mn^{III}bpy^{3+} + H_2O \rightleftarrows Mn^{III}_2O(bpy)_2^{4+} + 2H^+$$

The existence of a $Mn^{III}_2O(bpy)_2^{4+}$ intermediate can be inferred from the isolation in acetate buffer of the $[Mn^{III}_2O(AcO)_2(bpy)_2]^{2+}$.[46] Wieghardt et al.[47] proposed a mechanism for the disproportionation reaction which is favored by low pH:

(46) Matouzenko, G.; Albach, R. W.; Girerd, J.-J., unpublished results.
(47) Wieghardt, K.; Bossek, U.; Nuber, B.; Weiss, J.; Bonvoisin, J.; Corbella, M.; Vitols, S. E.; Girerd, J.-J. *J. Am. Chem. Soc.* **1988**, *110*, 7398–7411.

$$Mn^{III}{}_2O(bpy)_2{}^{4+} + H^+ \rightleftarrows Mn^{III}{}_2(OH)(bpy)_2{}^{5+}$$

$$Mn^{III}{}_2(OH)(bpy)_2{}^{5+} + Mn^{III}{}_2O(bpy)_2{}^{4+} \rightleftarrows Mn^{III,II}{}_2(OH)(bpy)_2{}^{4+} + Mn^{III,IV}{}_2O(bpy)_2{}^{5+}$$

Once $Mn^{III,IV}{}_2O(bpy)_2{}^{5+}$ is formed, it can react with the solvent and bpy to afford

$$Mn^{III,IV}{}_2O(bpy)_2{}^{5+} + H_2O \rightleftarrows Mn^{III,IV}{}_2O_2(bpy)_2{}^{3+} + 2H^+$$

$$Mn^{III,IV}{}_2O_2(bpy)_2{}^{3+} + 2bpy \rightleftarrows Mn^{III,IV}{}_2O_2(bpy)_4{}^{3+}$$

As shown by Cooper[25] and Crabtree,[48] the mixed-valence species can disproportionate to give

$$2Mn^{III,IV}{}_2O_2(bpy)_2{}^{3+} + H^+ \rightleftarrows MN^{III}{}_2O(OH)(bpy)_2{}^{3+} + Mn^{IV}{}_2O_2(bpy)_2{}^{4+}$$

This reaction is favored by low pH, as demonstrated by Brudvig et al.[42] The tendency of Mn^{IV} to aggregate is especially high, and trinuclear species $Mn^{IV}{}_3O_4(bpy)_4{}^{4+}$ have already been identified.[28,29] From the crystallographic studies of $Mn^{IV}{}_2O_2(bpy)_2(H_2PO_4)_2(HPO_4)$,[37] $Mn^{IV}{}_2O_2(bpy)_2(H_2O)_2AcO^{3+}$,[34] $Mn^{IV}{}_3O_4(bpy)_4{}^{4+}$,[28,29] and $Mn^{IV}{}_4O_6(bpy)_6{}^{4+}$, one identifies a common $Mn^{IV}{}_2O_2(bpy)_2{}^{4+}$ motif which has the geometry depicted in Figure 4. The bpy molecules are on the same side of the Mn_2O_2 motif and obey a C_2 axis perpendicular to Mn_2O_2. A tentative rationalization of the formation of the trinuclear and tetranuclear systems from the $Mn^{IV}{}_2O_2(bpy)_2{}^{4+}$ unit is proposed in Figure 4. The dotted atoms represent the points of attachment of the two dinuclear systems. Experimentally we found that the trinuclear and tetranuclear systems do not interconvert, and they appear to be the results of two different modes of association. The preferential formation of the trinuclear systems at low pH could be understood on the basis of the lowest availability of bpy at low pH.

Magnetic Susceptibility Measurements. The molar magnetic susceptibility χ_M was measured as a function of the temperature T. The results are shown in Figure 5 in the form of the $\chi_M T$ versus T plot. $\chi_M T$ decreases from 1.86 $cm^3\ mol^{-1}\ K$ at 294.1 K to 3.7 $10^{-3}\ cm^3\ mol^{-1}\ K$ at 12 K. This is characteristic of an antiferromagnetic coupling between the electronic spins of the Mn^{IV} ions which produces a spin $S = 0$ ground state. The structural information available on this compound allowed us to use the following Heisenberg Hamiltonian to analyze the data:

$$H_S = -J_{ab}S_aS_b - J_{bc}S_bS_c - J_{cd}S_cS_d$$

where $S_i = {}^3/_2$ is the value of the spin of the $Mn^{IV}{}_i$ in Figure 3. We took into account only nearest-neighbor interactions. We consider that there is no experimental information allowing a reliable estimate of the next-nearest-neighbors interactions.

Despite its simplicity, the topology of this cluster is such that there is no analytical solution for the eigenvalues since no subspin is a good quantum number. The only good quantum number is the total spin. The eigenvalues of H_S were calculated by diagonalizing the full 4^4 spin problem using the matrices built with $6j$ coefficients and the irreducible tensor theory. The magnetic susceptibility was calculated using Van Vleck's formula. Setting $g = 2$ for all four Mn^{IV} ions and $J_{ab} = J_{cd}$, the best fit was obtained for $J_{ab} = J_{cd} = -176\ cm^{-1}$ and $J_{bc} = -268\ cm^{-1}$ (Figure 5). The quality of the fit was not improved with J_{ab} and J_{cd} independent. Fits were also initialized by starting with $|J_{ab}| > |J_{cd}|$ but led to the former result.

(48) Sarneski, J. E.; Brzezinski, L. J.; Anderson, B.; Didiuk, M.; Manchanda, R.; Crabtree, R. H.; Brudvig, G. W.; Schulte, G. K. *Inorg. Chem.* **1993**, *32*, 3265–3269.

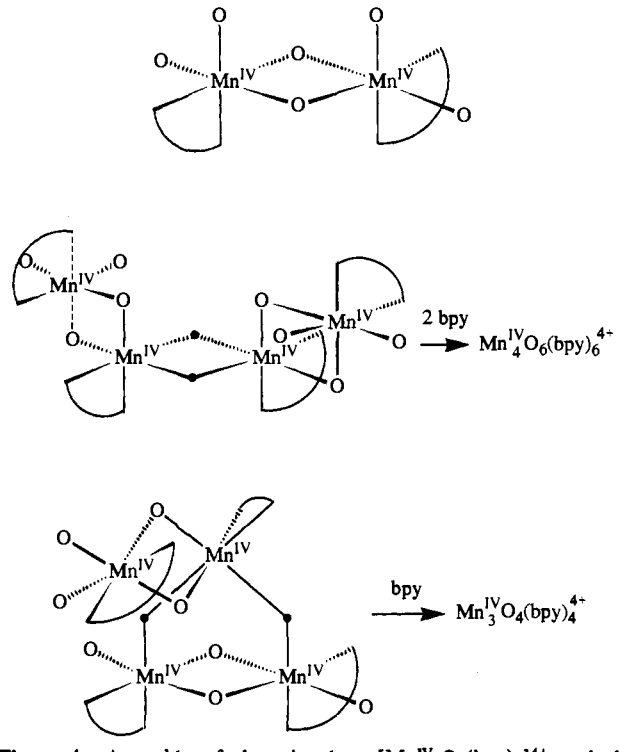

Figure 4. Assembly of the trinuclear $[Mn^{IV}{}_3O_4(bpy)_4]^{4+}$ and the tetranuclear $[Mn^{IV}{}_4O_6(bpy)_6]^{4+}$ systems from the dinuclear $[Mn^{IV}{}_2O_2(bpy)_2]^{4+}$ units.

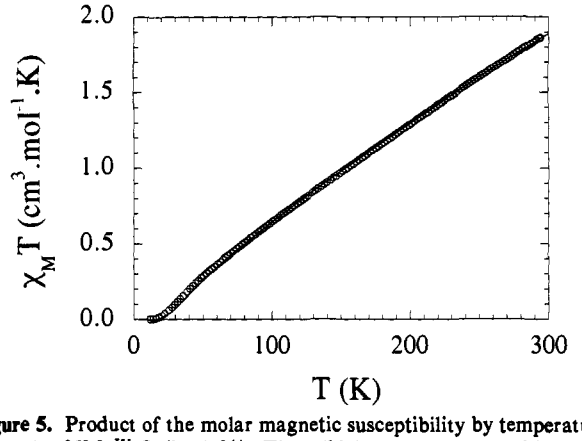

Figure 5. Product of the molar magnetic susceptibility by temperature per mole of $[Mn^{IV}{}_4O_6(bpy)_6]^{4+}$. The solid lines were generated from the best fit parameters given in the text.

The main components of the ground state $S = 0$ wave function are the wave functions $|m_a = -{}^3/_2, m_b = +{}^3/_2, m_c = -{}^3/_2, m_d = +{}^3/_2\rangle$ and $|m_a = +{}^3/_2, m_b = -{}^3/_2, m_c = +{}^3/_2, m_d = -{}^3/_2\rangle$, where m_i is the spin projection value of the local spin S_i. The wave function $|m_a = +{}^3/_2, m_b = -{}^3/_2, m_c = +{}^3/_2, m_d = -{}^3/_2\rangle$ can be depicted by the following diagram.

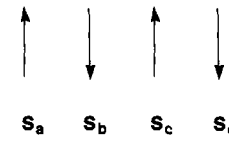

J_{bc} is found to be about 100 cm^{-1} more antiferromagnetic than J_{ab}. The Mn_b–Mn_c distance is slightly longer than Mn_a–Mn_b, which demonstrates that the antiferromagnetic coupling does not necessarily decrease when the metal–metal distance increases. The participation of the oxo bridges is certainly crucial. Along this line, it seems possible that the weakest J_{ab} coupling is due to the elongated O_{ab}–Mn_b distance.

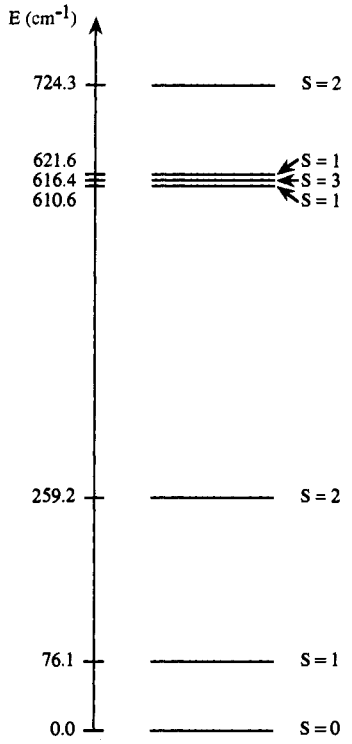

Figure 6. Lowest energy levels for $[Mn^{IV}_4O_6(bpy)_6]^{4+}$.

As far as J_{bc} is concerned, its value is comparable to the one found in $[Mn_2O_2(phen)_4]^{4+}$ ($J = -288$ cm^{-1}).[39] Libby et al.[49] have shown that replacement of nitrogen ligands by oxygen ones leads to a decrease in antiferromagnetic coupling ($J = -173$ cm^{-1} for picolinic acid in place of phen). This has been confirmed by Sarneski et al.[37] on a hydrogenophosphato complex which has a $J = -79$ cm^{-1}. Here the presence of oxo atoms has not the same effect. We have no explanation for this difference.

From the J_{ab} and J_{bc} experimentally determined values, the energy of the spin levels can be computed. The lowest levels are shown in Figure 6. The first excited state is a spin triplet ($S = 1$) state at 76.1 cm^{-1}. The next one is a spin quintet ($S = 2$) state at 259.2 cm^{-1}. Two triplet states and one septet then occur at around 600 cm^{-1}. If one ignores these two last triplets, the order $S = 0, 1, 2, 3$ is reminiscent of the result of the antiferromagnetic coupling of two $S_i = {}^3/_2$ ions. Quantitatively, this is not quite correct, since one would then expect the spin quintet at $3J = 76.1(3) = 228.3$ cm^{-1} and the spin septet at $6J = 456.6$ cm^{-1}. This peculiar organization of the lowest spin levels gives some insight on the physics of the coupling of four spins in a linear topology. Let us assume that the intermediate antiferromagnetic coupling $J_{bc} \neq 0$ and $J_{ab} = J_{cd} = 0$. The intermediate pair will be a spin singlet, and the terminal spins (S_a and S_d) will be uncoupled, i.e., the system will have four degenerate states; a singlet, a triplet, a quintet, and a septet. Now, suppose that the ratio J_{ab}/J_{bc} has a nonzero value but is $\ll 1$ (J_{ab} and J_{bc} both antiferromagnetic):

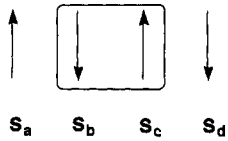

In this limit and for $J_{cd} = J_{ab}$, one can consider

$$H_S = H^0 + V$$

with the zeroth-order Hamiltonian $H^0 = -J_{bc}S_bS_c$ and the perturbation $V = -J_{ab}(S_aS_b + S_cS_d)$. It is possible to show by using second-order perturbation theory that then the lowest spin levels obey the Lande rule, with $J_{eff} = 2.5J_{ab}^2/J_{bc}$. *In this approximation, the terminal spins appear antiferromagnetically coupled through the almost diamagnetic intermediate pair.* This conclusion will be used below in the discussion of the OEC. In $[Mn^{IV}_4O_6(bpy)_6]^{4+}$, the agreement with the second-order perturbation theory is not quantitative since the ratio $J_{ab}/J_{bc} = 0.66$ is too large, but we saw that qualitatively this interpretation is correct.

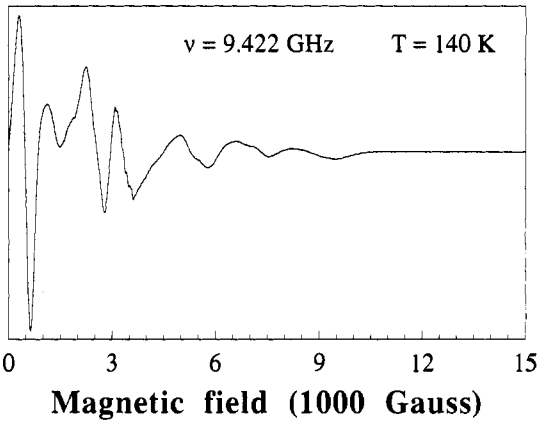

Figure 7. X-band EPR spectrum of $[Mn^{IV}_4O_6(bpy)_6]^{4+}$ on a powder sample.

EPR Spectra. The ground state of $[Mn^{IV}_4O_6(bpy)_6]^{4+}$ being a spin singlet, no EPR signal could be detected at helium temperature. From magnetic susceptibility data, we inferred that the first excited state is a spin triplet. Indeed, by raising the temperature, a signal appears at 40 K and is maximal at 130 K. Figure 7 shows the EPR spectrum recorded at 140 K on a powder sample. The pattern at $g = 2$ is due to a Mn^{II} impurity. A study as a function of frequency in X-band was tried to identify the resonances. It appears very likely that there are not only resonances from the triplet state but also from the quintet state. The observation of this signal suggests that it could be valuable to look for analogous resonances in the S_3 state of the OEC.

Electrochemistry. The main difficulty in this study was to avoid adsorption on working electrodes. The cyclic voltammogram in propylene carbonate is shown in Figure 8. In reduction, the wave is totally irreversible, showing unresolved peaks which could be attributed to very close successive reduction waves. Increase or decrease of the potential sweep rate does not modify the voltammogram. The peaks appear more clearly at 40 °C. On the first shoulder, a peak potential value of 0.20 V versus SCE can be deduced. From the comparison of the relative heights of the peaks, the first one would correspond to an intensity twice the value of the others. In oxidation, an anodic peak is observed at 1.20 V versus SCE before the wall of the solvent. The reversibility of the waves is very difficult to obtain, even at very high scan rate. In nitric acid solution at pH = 2.0, the cyclic voltammetry was not improved.

Preparative scale electrolytes followed by coulometry were conducted in nitric acid solution (pH = 2.0). We chose to reduce the complex at 0.50 V versus SCE just before the first reduction wave to attempt a single electron reduction. But the single electron reduction waves are so close that it was impossible to stop at the 1-electron reduced species. The integrated charge corresponded to 7.28 electrons. Decoloration of the solution and the EPR spectrum indicates that the final state is Mn^{II}. This suggests an 8-electron reduction:

$$[Mn^{IV}_4O_6(bpy)_6]^{4+} + 8e^- + 12H^+ \rightarrow 4Mn^{II} + 6bpy + 6H_2O$$

(49) Libby, E.; Webb, R. J.; Streib, W. E.; Folting, K.; Huffman, J. C.; Hendrickson, D. N.; Christou, G. *Inorg. Chem.* **1989**, *28*, 4037–4040.

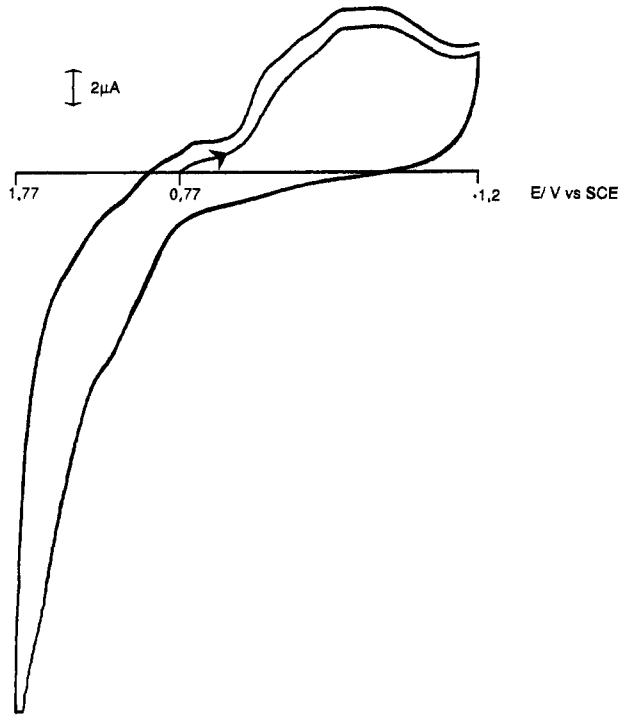

Figure 8. Cyclic voltammetry for $[Mn^{IV}_4O_6(bpy)_6]^{4+}$ in propylene carbonate.

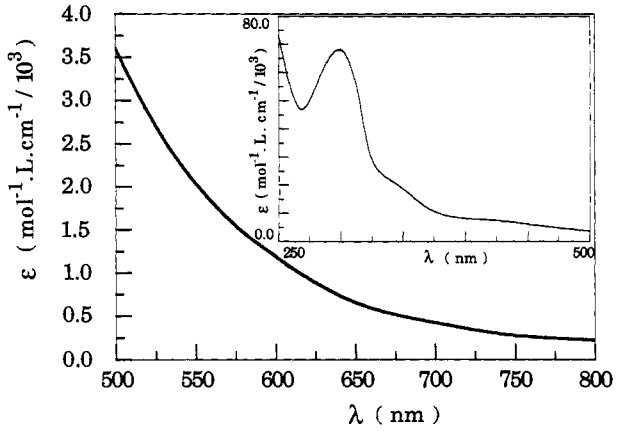

Figure 9. UV–vis in propylene carbonate.

After this reduction, the solution was oxidized at 1.40 V versus SCE (i.e., after the oxidation wave). 5.51 electrons were counted, which suggests a 6-electron oxidation:

$$4Mn^{II} \rightarrow 2(Mn^{III}Mn^{IV}) + 6e^-$$

Indeed, $[Mn^{III,IV}_2O_2(bpy)_4](ClO_4)_3$ precipitated.

The $[Mn^{IV}_4O_6(bpy)_6]^{4+}$ cluster is much less oxidizing than the $[Mn^{IV}_2O_2L_4]^{4+}$ species with L = phen, bpy (E^0 = 1.2 V versus SCE in acetonitrile).[25] An analogous observation has been reported for the trinuclear species $[Mn_3O_4(bpy)_4]^{4+}$ (reduction wave at 0.3 V versus SCE in acetonitrile).[29] At first sight, one could expect that the terminal sites $(bpy)_2Mn^{IV}O_2$ would be as oxidizing as the identical sites in the $[Mn^{IV}_2O_2L_4]^{4+}$ dinuclear units. Nevertheless, the 4+ charge is shared by more atoms in the tetranuclear than in the dinuclear systems. This can explain why these terminal sites $(bpy)_2Mn^{IV}O_2$ are much less oxidizing than the identical sites in the dinuclear units.

UV–Vis. The spectrum of the tetramer in an aqueous solution of HNO_3 (pH = 2.0) is represented in Figure 9. The absorption increases almost monotonously from 800 (220 M^{-1} cm^{-1}) to 300 nm (67 000 M^{-1} cm^{-1}). Poorly resolved peaks can be identified at 705 (14 184 cm^{-1}; 400 M^{-1} cm^{-1}), 602 (16 611 cm^{-1}; 1200 M^{-1} cm^{-1}), 430 (23 256 cm^{-1}; 7200 M^{-1} cm^{-1}), 346 (28 902 cm^{-1}, 20 000 M^{-1} cm^{-1}), and 300 nm (33 333 cm^{-1}, 67 000 M^{-1} cm^{-1}). Mn^{IV} d-d bands in Mn-oxo complexes have been studied in particular in ref 50. The following transitions have been attributed: 11 600 cm^{-1} ($^4A_2 \rightarrow {}^2T$), 18 000 cm^{-1} ($^4A_2 \rightarrow {}^4T_2$-(a)), 22 800 cm^{-1} ($^4A_2 \rightarrow {}^4T_2$(b)). This last transition may be the one observed here at 430 nm (23 256 cm^{-1}). The $^4A_2 \rightarrow {}^4T_2$(a) transition may be the one observed at 602 nm (16 611 cm^{-1}). The lack of resolution in this spectrum is due to the presence of two types of chromophores: $Mn^{IV}N_4O_2$ and $Mn^{IV}N_2O_4$. In ref 50, the Mn^{IV}-oxo LMCT bands have been identified in $[Mn^{III}O_2Mn^{IV}]^{3+}$ systems. They are numerous and distributed from wavenumbers as small as 6500 cm^{-1} to as large as 31 000 cm^{-1}. In this present tetranuclear system, a large number of these bands are expected. They are at the origin of the absorption in a large spectral band observed here.

Relevance to the OEC. In the following we will compare $[Mn^{IV}_4O_6(bpy)_6]^{4+}$ to the OEC. Discussion relies on two current hypotheses based on experimental results: (i) in S_2, the oxidation states are $Mn^{IV}_3Mn^{III}$ [3] and (ii) the structure of the OEC is basically the one proposed by Klein et al.[3] (Figure 1). The manganese atoms are labeled abcd.

In this framework, $[Mn^{IV}_4O_6(bpy)_6]^{4+}$ can be looked at as a model of the S_3 state. This can well be only formal as far as the oxidation states are concerned, since it is considered as possible that in the step $S_2 \rightarrow S_3$, the manganese of the OEC would not be oxidized.[2] Regardless, the $[Mn^{IV}_4O_6(bpy)_6]^{4+}$ cation offered us the possibility to study the spin coupling problem in a chain tetranuclear system. These results will now be applied to the OEC since Klein's model implies a chain topology for the spin coupling problem in the natural system. We will study the S_2 state since it is better known.[2] Two S_2 states were distinguished on the basis of EPR, one with $g = 2$ and another with $g = 4.1$. The $g = 2$ signal has been attributed to a spin doublet ground state of the cluster.[6] The $g = 4.1$ signal has been considered as originating from a $S = {}^3/_2$[11-13] or a $S = {}^5/_2$[14] ground state.

(a) The $g = 2$ State. There are two distributions of oxidation states, (IV,III,IV,IV) or (III,IV,IV,IV), along the abcd cluster of Figure 1. The first one implies $[Mn^{IV}_aMn^{III}_bX_2]^{3+}$, $[Mn^{III}_b$-$Mn^{IV}_cX]^{5+}$, and $[Mn^{IV}_cMn^{IV}_dX_2]^{4+}$ subunits (X = O or OH). From model studies, J_{ab}, J_{bc}, and J_{cd} are then all negative. If one considers only nearest-neighbor interactions, the ground state is evidently a spin doublet, the main component of which will be $|m_a = +{}^3/_2, m_b = -2, m_c = +{}^3/_2, m_d = -{}^3/_2\rangle$ (see Table 3a). The second distribution of oxidation states implies $[Mn^{III}_aMn^{IV}_bX_2]^{3+}$, $[Mn^{IV}_bMn^{IV}_cX]^{6+}$, and $[Mn^{IV}_cMn^{IV}_dX_2]^{4+}$. Again from model studies, J_{ab} and J_{cd} will be likely negative. J_{bc} can be positive or negative,[47,51] but whatever this sign may be, the ground state will be $S = {}^1/_2$ with as main component either $|+2, -{}^3/_2, +{}^3/_2, -{}^3/_2\rangle$ ($J_{bc} < 0$) or $|+2, -{}^3/_2, -{}^3/_2, +{}^3/_2\rangle$ ($J_{bc} > 0$) (see Table 3b). Thus, the spin doublet S_2 state can easily be understood within Klein's model.

(b) The $g = 4.1$ State. (i) Linear Models. The $g = 4.1$ form of the S_2 state has a ground state of spin higher than $S = {}^1/_2$. With the previous hypotheses, it is possible to get $S > {}^1/_2$ (see Table 3). *Note that with this linear topology, the Mn_4 cluster cannot have a ground state with $S = {}^3/_2$.* A ground state with spin $S = {}^5/_2$ is possible with the arrangements $(+2, -{}^3/_2, -{}^3/_2, -{}^3/_2)$ or $(+{}^3/_2, -2, +{}^3/_2, +{}^3/_2)$, but these imply that the $[Mn^{IV}_c$-$Mn^{IV}_dX_2]^{4+}$ pair must be ferromagnetically coupled, which is unknown chemically. The $g = 4.1$ signal is thus difficult to reconcile with the model of Figure 1.

The only possible way to get a $S = {}^5/_2$ ground state compatible with the current magnetochemistry of the models is to modify the

(50) Gamelin, D. R.; Kirk, M. L.; Stemmler, T. L.; Pal, S.; Armstrong, W. H.; Penner-Hahn, J. E.; Solomon, E. I. *J. Am. Chem. Soc.* **1994**, *116*, 2392–2399.

(51) Hagen, K. S.; Westmoreland, T. D.; Scott, M. J.; Armstrong, W. H. *J. Am. Chem. Soc.* **1989**, *111*, 1907–1909.

Table 3. Spin of the Ground State for the Linear Spin Problem as a Function of the Sign of the Coupling Parameters[a]

sign of J_{ab}	sign of J_{bc}	sign of J_{cd}	S_{GS}	spin organization along *abcd*
		(a) Mn^{IV}_a, Mn^{III}_b, Mn^{IV}_c, Mn^{IV}_d Case		
–	–	–	$^1/_2$	$(+^3/_2, -2, +^3/_2, -^3/_2)$
–	+	–	$^1/_2$	$(+^3/_2, -2, -^3/_2, +^3/_2)$
–	–	+	$^5/_2$	$(+^3/_2, -2, +^3/_2, +^3/_2)$
–	+	+	$^7/_2$	$(+^3/_2, -2, -^3/_2, -^3/_2)$
+	+	–	$^7/_2$	$(+^3/_2, +2, +^3/_2, -^3/_2)$
+	–	–	$^7/_2$	$(+^3/_2, +2, -^3/_2, +^3/_2)$
+	+	+	$^{13}/_2$	$(+^3/_2, +2, +^3/_2, +^3/_2)$
+	–	+	$^1/_2$	$(+^3/_2, +2, -^3/_2, -^3/_2)$
		(b) Mn^{III}_a, Mn^{IV}_b, Mn^{IV}_c, Mn^{IV}_d Case		
–	–	–	$^1/_2$	$(+2, -^3/_2, +^3/_2, -^3/_2)$
–	+	–	$^1/_2$	$(+2, -^3/_2, -^3/_2, +^3/_2)$
–	–	+	$^7/_2$	$(+2, -^3/_2, +^3/_2, +^3/_2)$
–	+	+	$^5/_2$	$(+2, -^3/_2, -^3/_2, -^3/_2)$
+	+	–	$^7/_2$	$(+2, +^3/_2, +^3/_2, -^3/_2)$
+	–	–	$^7/_2$	$(+2, +^3/_2, -^3/_2, +^3/_2)$
+	+	+	$^{13}/_2$	$(+2, +^3/_2, +^3/_2, +^3/_2)$
+	–	+	$^1/_2$	$(+2, +^3/_2, -^3/_2, -^3/_2)$

[a] The majority component of the spin wave function of the ground state is indicated.

structural proposal of Figure 1 into the "short-short-long" model (Figure 10a), which from chemical models could have $J_{ab} < 0$, $J_{bc} < 0$, $J_{cd} > 0$ and a $S = {}^5/_2$ state with $|+^3/_2, -2, +^3/_2, +^3/_2\rangle$ as the main component. In this model, the spin of the ground state of the Mn_4 cluster could easily change from $S = {}^5/_2$ to $^1/_2$ by just changing J_{cd} from ferromagnetic to antiferromagnetic. Importantly, the change of sign of the spin coupling in a Mn^{IV}–O–Mn^{IV} unit has been shown by Armstrong et al.[51] to occur by protonation of the bridging oxo group. A change of position of the valence III from b to c could also achieve a change in spin state.

(ii) The Ring Model. We would like now to show that introducing a ferromagnetic link J_{da} between the two terminal Mn atoms (a and d) of Klein's model makes possible a ground state with a spin $^1/_2$ or higher than $^1/_2$. Let us suppose that, as in the title tetranuclear complex, J_{ab}, J_{bc}, and J_{cd} in the model of Figure 1 are negative and that a (III,IV,IV,IV) distribution exists along the abcd sites.[52] The ground state will be a $S = {}^1/_2$ state (main component, $|+2, -^3/_2, +^3/_2, -^3/_2\rangle$) as explained above. From our study of $[Mn^{IV}_4O_6(bpy)_6]^{4+}$, we understood that even with substantial J_{ab}, J_{bc}, and J_{cd} coupling constants, the S_a and S_d spins can be only weakly antiferromagnetically coupled. *In this case, introduction of a ferromagnetic coupling between S_a and S_d can tilt these two spins to bring a higher spin state as the ground state.* To check quantitatively this proposal, we solved exactly the ring Hamiltonian

$$H_S = -J_{ab}S_aS_b - J_{bc}S_bS_c - J_{cd}S_cS_d - J_{da}S_dS_a$$

corresponding to the model of Figure 10b. Such a ring model has already been studied by Kirk et al.[53] and Kusonoki.[7] In ref 7, the $Mn^{III}Mn^{IV}$ pair was supposed to be in the $S = {}^1/_2$ state, which is not a requisite here.

The ground states of this model were explored with J_{ab} and J_{cd} set equal to –1 (arbitrary unit), J_{da} varied between 0 and +1, and J_{bc} varied between –5 and 0. The results are represented in Figure 11 in the form of a phase diagram. We see horizontal and vertical frontiers between $S = {}^1/_2$ and $^3/_2$ ground states. When $J_{bc} > -0.6$, the $S = {}^1/_2$ is the ground state: for J_{da} small the system can be approached as two AF dimers ($S_{ab} = {}^1/_2$, $S_{cd} = 0$). As soon as J_{bc} is equal to –0.6, the decoupling of the terminal spins becomes efficient, and it is feasible to tilt them with a reasonable value of J_{da}. For $J_{bc} = -1$, a $J_{da} = +0.35$ is enough to bring down a $S = {}^3/_2$ state. If $J_{ab} = -1.00$ cm^{-1}, this means $J_{da} = +35$ cm^{-1}. A $S = {}^5/_2$ ground state is also possible (for instance, for $J_{ab} = J_{cd} = -1$, $J_{bc} = -2$, $J_{da} = +0.5$). A J(mono-μ-oxo)/J(di-μ-oxo) ratio of 0.6 or larger is not unrealistic. For instance, this ratio is 0.63 in $[Mn^{IV}_3O_4(bpy)_4Cl_2]^{2+}$ [28] and 0.54 in $[Mn^{IV}_3O_4(bpy)_4(H_2O)_2]^{2+}$.[29] It is not clear how an interaction between a Mn^{III} and a Mn^{IV} ion can be ferromagnetic, but it cannot be ruled out. One has to keep in mind that beyond the usual mechanism for ferromagnetic interaction, there exists a mechanism specific to mixed valence pairs which is called double exchange. In fact, double exchange was discovered by physicists on $Mn^{III}Mn^{IV}$ manganites,[54] which are perovskites with ferromagnetic Mn^{III}–

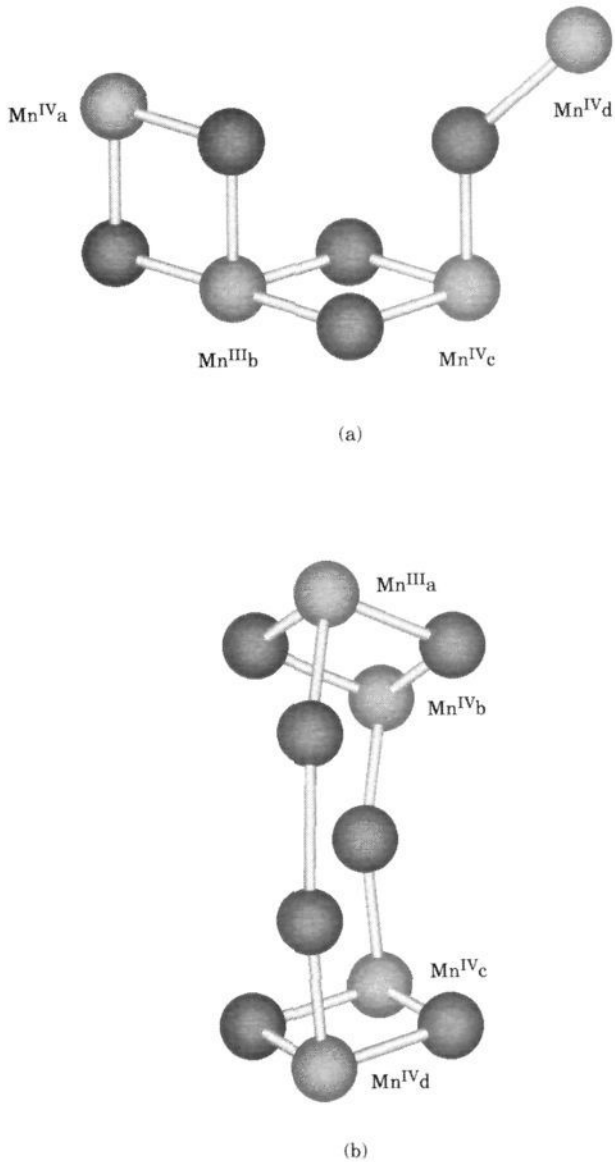

Figure 10. Structural models for the OEC. (a) The "short–short–long" model for the S_2 state. This model is possible only if the $g = 4.1$ signal arises from a $S = {}^5/_2$ ground state. (b) Ring version of Klein's model, J_{da} has to be >0 (ferromagnetic interaction) to explain the $S = {}^3/_2$ or $^5/_2$ ground state. Mn–O distances have been taken equal to 1.8 Å; two Mn–Mn distances are equal to 2.7 Å and a third one is equal to 3.3 Å. In b, we have assumed that axial O atoms are linked to the terminal Mn atoms; the distance in this model between these axial O atoms is 2.16 Å. This is hypothetical, and atoms other than O could occupy these positions. The line between these O atoms does not stand for a bond but symbolizes *the J_{ad} magnetic interaction.*

(52) The (IV,III,IV,IV) distribution was studied, too, but stabilization of a high-spin ground state necessitates a larger J_{da} value and is thought less favorable.

(53) Kirk, M. L.; Chan, M. K.; Armstrong, W. H.; Solomon, E. I. *J. Am. Chem. Soc.* **1992**, *114*, 10432–10440.

(54) de Gennes, P. G. *Phys. Rev.* **1960**, *118*, 141–154 and references therein.

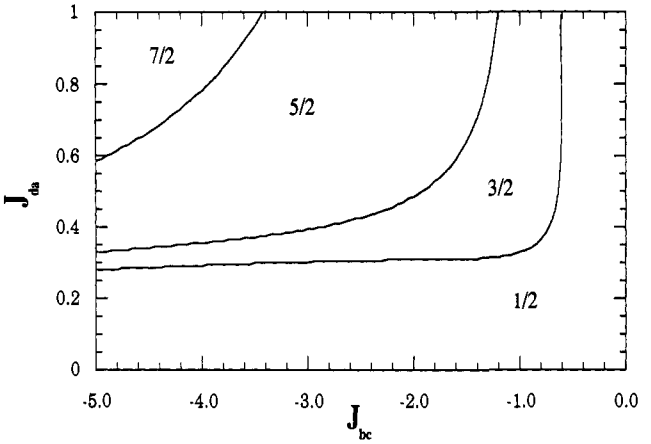

Figure 11. Nature of the ground state of the ring spin problem as a function of J_{da} and J_{bc}, with $S_a = 2$, $S_b = {}^3/_2$, $S_c = {}^3/_2$, $S_d = {}^3/_2$, $J_{ab} = J_{cd} = -1$ (arbitrary unit). Note the linear frontiers between $S = {}^1/_2$ and $S = {}^3/_2$.

O–Mn^{IV} units.[55] The passage from the $g = 4.1$ S_2 state to the $g = 2$ S_2 state would be related to a slight change in J_{da} or J_{bc}.

Conclusion

We isolated and structurally characterized the new linear tetramer $[Mn^{IV}_4O_6(bpy)_6]^{4+}$. This species is stable in aqueous solution at pH = 2. The electrochemistry showed that this entity is much less oxidizing than the dinuclear $[Mn^{IV}_2O_2L_4]^{4+}$ (L = bpy, phen) species. This seems to be due to the spread of the 4+ charge. Moreover, reduction destroyed the complex and went to $4Mn^{II}$. Magnetic susceptibility measurements indicated strong antiferromagnetic couplings between Mn^{IV} ions. The organization of the lowest spin levels can be reproduced approximately by a Heisenberg coupling between the two terminal Mn^{IV} ions with $J_{eff} = 2.5J_{ab}^2/J_{bc}$. This led to the idea that in this tetramer, the two terminal atoms are antiferromagnetically coupled via a quasi diamagnetic core made of the central Mn_2O_2 unit.

To our knowledge, the title cation $[Mn^{IV}_4O_6(bpy)_6]^{4+}$ is the closest model to Klein's model of the OEC, although there are two bridging oxo groups in $[Mn^{IV}_4O_6(bpy)_6]^{4+}$ versus one proposed in the OEC.

In both Klein's model and $[Mn^{IV}_4O_6(bpy)_6]^{4+}$, the spin coupling problem has a chain topology. We therefore compared both systems with the additional hypothesis that in the S_2 state, the oxidation state is $Mn^{IV}_3Mn^{III}$, which is substantiated by XANES studies.

We found that the model of Figure 1 is not able to explain both the multiline $g = 2$ and the $g = 4.1$ signals, and we proposed two modified versions which are free from this discrepancy. We insisted on the importance of the understanding of the origin of the S_2 $g = 4.1$ signal to decide between these two models. Magnetization studies of the OEC could contribute to the resolution of this dilemma. Simulations of the EPR signals can also contribute to the debate over the validity of these models.

Acknowledgment. We acknowledge Dr. J.-L. Zimmermann for assistance in recording the EPR spectra.

Supplementary Material Available: Tables of positional and thermal parameters, interatomic distances and angles, and anisotropic temperature factors (9 pages); observed and calculated structure factors (5 pages). This material is contained in many libraries on microfiche, immediately follows this article in the microfilm version of the journal, and can be ordered from the ACS; see any current masthead page for ordering information.

(55) Interestingly, one can note that in the structure in Figure 10b, the extra unpaired electron on Mn^{III}_a is in a d_{z^2} orbital pointing toward Mn^{IV}_d which could favor some amount of delocalization and thus double exchange ferromagnetic interaction.